The P2 nucleic acid binding protein of sugarcane bacilliform virus is a viral pathogenic factor

Xiongbiao Xu[1#*], Yinian Lou[1#], Kaili Liang[1], Jingying Liu[1], Zhiyuan Wang[1], Baoshan Chen[1], Wenlan Li[2]

[1] State Key Laboratory for Conservation and Utilization of Subtropical Agro-bioresources, Guangxi key Laboratory of Sugarcane biology, College of Agriculture, Guangxi University, Nanning, Guangxi, P.R. China
[2] College of Life Science and Technology, Guangxi University, Nanning, Guangxi, P.R. China

* Corresponding Author:
Xiongbiao Xu[1]
No.100, East Daxue Road, Nanning, Guangxi Province, 530004, P.R. China
Email address: xiongbiaox@gxu.edu.cn

Abstract

Background. *Saccharum spp.* is the major source of sugar and plays significant roles in global renewable bioenergy. Sugarcane bacilliform virus (SCBV) is one of the most important viruses infecting sugarcane, causing severe yield losses and quality degradation. It is of great significance to reveal the pathogenesis of SCBV and resistance breeding. However, little is known about the viral virulence factors or RNA silencing suppressors and the molecular mechanism of pathogenesis.

Methods. To systematically investigate the functions of the unknown protein P2 encoded by SCBV ORF2. Phylogenetic analysis was implemented to infer the evolutionary relationship between the P2 of SCBV and other badnaviruses. The precise subcellular localization of P2 was verified in the transient infiltrated *Nicotiana benthamiana* epidermal mesophyll cells and protoplasts by using the Laser scanning confocal microscope (LSCM). The post-transcriptional gene silencing (PTGS) and transcriptional gene silencing (TGS) RNA silencing suppressor activity of P2 was analysed, respectively. And the probable mechanism of P2 on repressing DNA methylation was verified by restriction digestion and RT-qPCR. To explore the pathogenicity of P2, a potato virus X-based viral vector was used to heterologously express SCBV P2, and the consequent H_2O_2 accumulation was detected by 3,3'-diaminobenzidine (DAB) staining method.

Results. Phylogenetic analysis shows that SCBV has no obvious sequence similarity and low genetic relatedness to *Badnavirus* and *Tungrovirus* representatives. LSCM studies show that P2 is localized in both the cytoplasm and nucleus. Moreover, P2 is shown to be a suppressor of PTGS and transcriptional gene silencing TGS, which can not only repress ssRNA-induced gene silencing but also disrupt the host RNA-directed DNA methylation (RdDM) pathway. In addition, P2 can

40 trigger an oxidative burst and cause typical hypersensitive-like response (HLR) necrosis in
41 systemic leaves of *N. benthamiana* when expressed by PVX. Overall, our results laid a foundation
42 for deciphering the molecular mechanism of SCBV pathogenesis and made progress for resistance
43 breeding.

44 **Keywords:** Sugarcane bacilliform virus, phylogenetic relationship, pathogenic factor, RNA
45 silencing suppressor, hypersensitive-like response.

Introduction

47 *Saccharum spp.* is a primary sugar-producing crop and an important industrial renewable
48 bioenergy crop, which is cultivated throughout the world's tropical and subtropical areas.
49 Sugarcane bacilliform virus (SCBV) is one of the primary viruses infecting sugarcane and causing
50 severe damage. It was first identified in cultivar B34104 in Cuba in 1985 (Geijskes et al., 2002),
51 and later purified from cultivar Mex.57-473 (Lockhart, 1988). SCBV is spontaneously spread by
52 the insect vectors *Dysmicoccus boninsis* and *Saccharicoccus sacchari*. It can also be transmitted
53 experimentally by raw viral sap or by Agrobacterium-mediated inoculation (Lockhart et al., 1995),
54 but failed to be transmitted by mechanical friction. In addition, long-distance spread of virus-
55 infected materials is an important means of transmission. SCBV has a relatively broad host range,
56 including *Sorghum halepense*, *Brachiaria* sp., *Rottboellia exaltata*, *Panicum maximum*, and
57 experimental hosts such as *Oryza sativa* and *Musa* sp. (Bouhida et al., 1993; Lockhart et al., 1995;
58 Viswanathan et al., 1996). Usually, the visible symptoms caused by SCBV are mottling, stunted
59 growth, chlorotic streaks, and internode fracture (Viswanathan et al., 1996). Once infection, the
60 sugarcane plants show varying degrees of reduced juice yield, sugar content, gravity purity and
61 stem weight, resulting in significant yield and quality losses (Ahmad et al., 2019). Occasionally,
62 masked symptoms occur due to temperature, drought, nutritional conditions changes. Moreover,
63 much more complicated symptoms could be found due to co-infection with other viruses (Lockhart
64 et al., 1995; Singh et al., 2009; Viswanathan and Premachandran, 1998).

65 SCBV belongs to the genus *Badnavirus* (family *Caulimoviridae*), with bacilliform, non-
66 enveloped virions of 130-150 nm in length and 30 nm in diameter (Bhat et al., 2016; Bouhida et
67 al., 1993; Lockhart, 1988), containing a circular, covalent, discontinuous dsDNA genome of
68 approximately 7.5-8.0 kilobases (Kb), which generally encodes three open reading frames (ORFs).
69 The exact roles of ORF1 and ORF2 have not been confirmed, and ORF3 has been found to encode
70 a large polyprotein truncated into movement protein (MP), coat protein (CP), aspartic protease
71 (AP), reverse transcriptase (RT) and ribonuclease H (RNase H), but the precise cutting sites remain
72 unknown (Geijskes et al., 2002; Sun et al., 2016). Previous studies have suggested that a short
73 fragment between the 3'-end of ORF3 and ORF1 may act as a strong promoter in both monocot
74 and dicot species (Davies et al., 2014; Gao et al., 2017). The P2 protein of Commelina yellow
75 mottle virus (CoYMV) has been shown to be involved in virion particle assembly (Cheng et al.,
76 1996), and the P2 protein encoded by Cacao swollen shoot virus (CSSV) can bind to cognate or
77 heterologous DNA as well as ssRNA, and the C-terminus appears to be essential for nucleic acid
78 binding (Jacquot et al., 1996). Jacquot and colleagues have demonstrated that the proline-rich
79 region ($_{99}$-PPKKGIKRKYPA-$_{110}$) at the C-terminal of Rice tungro bacilliform virus (RTBV) P2

80   plays an important role in the interaction between P2 and nucleic acids (Jacquot et al., 1997). All
81   these results provide the basis for studying the function of the P2 protein of *Badnavirus*, but little
82   is known about its roles in viral pathogenicity.

83   In this study, the complete genome of SCBV was deciphered and the functions of its encoded
84   P2 protein were analyzed. The P2 protein was found to share low sequence similarity with other
85   badnaviruses and elicit a hypersensitive-like response and suppress posttranscriptional and
86   transcriptional gene silencing, suggesting that P2 is a viral pathogenicity factor. Our findings
87   increase our understanding of the pathogenesis of SCBV virus and lay a foundation for antiviral
88   resistance breeding.

89

Materials & Methods

91   **Source of plant materials.** Sugarcane plants of the Badila cultivar that exhibited mottling,
92   stunting, and chlorotic streaking symptoms were collected from Menghai County, Yunnan
93   Province, China, and rapidly frozen in liquid nitrogen and then stored at -80 ℃.

94   **Multiple alignment and phylogenetic analyses.** Amino acid sequence similarities were
95   determined for the P2 of 6 representative members of the genus *Badnavirus* and the sole member
96   of *Tungrovirus* (Rice tungro bacilliform virus, RTBV), all sequences and GenBank accession
97   numbers are listed in Table 1. Sequence multiple alignment was performed with the MegAlign
98   program using the DNASTAR software. The corresponding sequences of the above viruses were
99   aligned, and percent identities were determined in Clustal W. The phylogenetic tree was inferred
100   via the Neighbor-joining method in MEGA11 with the bootstrap 1, 000 replicates.

101   **Construction of plasmids.** Total genomic DNA was extracted using cetyltrimethylammonium
102   bromide (CTAB)-based methods as previously described (Springer, 2010). Genomic DNA was
103   purified after RNase A digestion and used as a template for PCR. The complete genome of SCBV
104   was obtained by isothermal amplification with Phi29 MAX DNA Polymerase (Cat#: N106-01,
105   Vazyme, Nanjing, China) according to the manufacturer's instructions. The products of isothermal
106   amplification were then used as templates for amplification of the complete genome using primer
107   pair SCBV/F and SCBV/*Sma*I/R (Table S1) and Phanta EVO HS Super-Fidelity DNA Polymerase
108   (Cat#: P504-d1, Vazyme, Nanjing, China). The SCBV complete genome sequence was then
109   subcloned into the pCE2-TA/Blunt-Zero vector (Cat#: C601-01, Vazyme, Nanjing, China) and
110   transformed into *Escherichia coli* Top10. The positive colonies were cultured and verified by PCR
111   and Sanger sequencing. The complete genome of SCBV was then submitted to National Center
112   for Biotechnology Information (GenBank accession number: OR672147). The ORF2 coding
113   sequence was amplified by PCR and cloned into PVX-based vector pGR106 by digested with *Cla*I
114   and *Sal*I followed by T4 DNA ligase (Cat#: EL0014,ThermoFisher Scientific, Shanghai, China)
115   ligation to get the recombinant plasmid PVX-P2. Also, P2 was inserted to the pCHF3 binary
116   expression vector or fused to the N-terminal of enhanced green fluorescent protein (eGFP) in
117   pCHF3-eGFP by double enzyme digestion with S*ac*I/*Bam*HI,. The corresponding recombinant
118   plasmids were referred to as pCHF3-P2 and pCHF3-P2-eGFP, respectively. All primers used in
119   this study are listed in Supplementary Table S1.

Plant growth and agroinoculation. Wild-type, 16c (Voinnet and Baulcombe, 1997), 16-TGS (Raja et al., 2008) and RFP-H2B transgenic seedlings of *N. benthamiana* were grown to the 4- to 5-leaf stage in an insect-free chamber at a constant temperature of 25 °C and a 16-h/8-h day/night cycle. The binary plasmids pCHF3-P2 and empty pCHF3 were transfected into *Agrobacterium tumefaciens* strain EHA105, and the recombinant plasmids PVX and PVX-P2 were transformed into *A. tumefaciens* GV3101 by electroporation. Suspensions of *A. tumefaciens* cultures were regulated to OD_{600} of 1.0, and the Agrobacterium containing PVX-P2 was infiltrated into *N. benthamiana* wild-type or 16-TGS seedlings using a 1-mL syringe without a needle. Transient PTGS suppression experiments were conducted as previously described (Johansen and Carrington, 2001; Li et al., 2014; Li et al., 2015).

Plant transformation. The transgenic *N. benthamiana* plants over-expressing P2 or empty vector were generated by using the Agrobacterium-mediated leaf disc transformation method. The binary empty vector pCHF3 or recombinant plasmid pCHF3-P2 were transformed into *A. tumefaciens* strain EHA105, and used for transfection of *N. benthamiana* leaf discs. Potential transformants were selected on MS media containing 200 μg ml^{-1} cefotaxime and 200 μg ml^{-1} kanamycin. Kanamycin-resistant cluster buds were cut off, placed on rooting media, cultured to a height of 5-6 cm, and then transplanted into soil. Transgenic seedlings were verified by PCR with CaMV 35S promoter or P2 specific primers, respectively. Relative levels of P2 mRNA in transgenic plants were confirmed by RT-qPCR.

H_2O_2 detection in plants. H_2O_2 production was detected visually in *N. benthamiana* leaves using the 3,3'-diaminobenzidine (DAB) staining method (Cat#: A690009, Sangon Biotech, Shanghai, China) (Sharma and Ikegami, 2010) and making some modifications as previously described (Liang et al., 2023).

Subcellular localization analysis. For subcellular localization experiments, fluorescence in RFP-H2B transgenic *N. benthamiana* leaf epidermal cells or protoplasts inoculated with pCHF3-eGFP- and pCHF3-P2-eGFP was examined by confocal microscopy (Leica TCS SP8MP, Mannheim, Germany) 2- to 3-days post inoculation (dpi) as described (Shen et al., 2011; Yoo et al., 2007).

Protoplast preparation. To further observe the more precise subcellular localization of SCBV P2 protein, the protoplasts of RFP-H2B transgenic *N. benthamiana* leaf epidermal cells were prepared by digesting with 1.5% (wt/vol) cellulase (Cat#: A002610, Sangon Biotech, Shanghai, China) and 0.4% (wt/vol) macerozyme R10 (Cat#: A004297, Sangon Biotech, Shanghai, China) as described (Yoo et al., 2007).

DNA methylation analysis by restriction digestion. Genomic DNA of pCHF3 and P2 transgenic plants was extracted by using the CTAB method. Digestion analysis of genomic DNA was performed by using a methylation-insensitive restriction endonuclease *Bam*HI (Cat#: FD0054, ThermoFisher Scientific, Shanghai, China) and a methylation-dependent endonuclease *Mcr*BC (Cat#: M0272, New England Biolabs, Ipswich, MA, USA). The restriction digestion reaction (50 μl) consists of 10 μg of genomic DNA, 50 U of the respective endonuclease according to the manufacturer's specifications. Digested products were instantly separated by electrophoresis through a 1.5% agarose gel.

160 **RT-qPCR.** RT-qPCR analysis was performed to measure the transcription level of core genes in
161 the RNA-directed DNA methylation (RdDM) pathway. Total RNAs from PVX-inoculated *N.*
162 *benthamiana* and P2 or empty vector-transgenic *N. benthamiana* plants were extracted as
163 experimental and control groups using RNAiso Plus reagent (Cat#: 9108, Takara, Beijing, China)
164 and the A_{260}/A_{280} value and concentration of RNA products were measured by NanoPhotometer®
165 N60/N50 (IMPLEN, Germany). 2 µg of high-quality RNA were converted to cDNA using HiScript
166 III 1st Strand cDNA Synthesis Kit (+gDNA wiper) (Cat#: R312-01, Vazyme, Nanjing, China)
167 according to the manufacturer's instructions. The cDNA product was diluted 10-fold and served
168 as a template for RT-qPCR. Each reaction mixture contained 2 µL of the diluted cDNA, 10 µL of
169 2 × ChamQ Universal SYBR qPCR Master Mix (Cat#: Q711-02, Vazyme, Nanjing, China), 0.4
170 µL of each of the forward and reverse primer (10 µM) in a total volume of 20 µL (primers are
171 listed in Table S1). Three independent biological and experimental replicates were performed and
172 the reactions were run under the following program conditions: 95 ℃ for 30 sec, and 40 cycles of
173 95 ℃ for 10 sec and 60 ℃ for 30 sec. Melting curves were derived (95 ℃ for 15 sec, 60 ℃ for 60
174 sec and 95 ℃ for 15 sec) for each reaction to ensure a single product. Reactions were performed
175 using the LightCycler 96 real-time PCR system (F. Hoffmann-La Roche Ltd. Switzerland). The
176 qPCR data was analyzed by using the $2^{-\triangle\triangle Ct}$ method (Livak and Schmittgen, 2001). All primers
177 used for qRT-PCR detection in this study are listed in Supplementary Table S1.
178 **Immunoblotting.** Total protein of systemic leaves was extracted from PVX-infected plants as
179 described previously (Xiong et al., 2009). Immunoblotting was performed with primary Mouse
180 anti-PVX CP monoclonal antibodies, followed by HRP-conjugated Goat Anti-Mouse IgG (Cat#:
181 D110087, Sangon Biotech, Shanghai, China). Blotted membranes were washed thoroughly and
182 visualized using the SuperPico ECL Chemiluminescence Kit according to the manufacturer's
183 protocol (Cat#: E422, Vazyme, Nanjing, China).
184

185 # Results

186 **Phylogenetic relationships between SCBV P2 and other taxa of the genus Badnavirus**
187 The complete genome of SCBV was sequenced and submitted to NCBI (GenBank accession
188 number: OR672147). The ORF2 of SCBV is 372 nucleotides (nt) long and encodes a small protein
189 of 123 amino acids (aa) called P2. The complete amino acid sequences of SCBV P2, Rice tungro
190 bacilliform virus (RTBV, GenBank accession number: AAD30189), and several representative
191 members of the genus *Badnavirus* (as seen in Table 1) were aligned and phylogenetic analyzed.
192 Multiple sequence alignment shows that all P2 amino acid sequences have no obvious sequence
193 similarity (Fig. 1A, Table 1). A coiled-coil-like domain ($_{47}$-
194 LLTLHGKITALEGRLQDLKEDIAKKADK-$_{74}$) was predicted in SCBV P2 by InterPro online
195 prediction (https://www.ebi.ac.uk/interpro/). The coiled-coil like domain is quite conservative in
196 length and position in all the above viruses (Fig. 1A). Phylogenetic analysis shows that all the 8
197 viruses were clustered into three groups, and SCBV P2 was assigned in a clade alone and had a
198 relatively closer relationship with Banana streak OL virus and Cycad leaf necrosis virus P2, and
199 these three viruses were clustered in the same group (Fig. 1B).We have previously demonstrated

200 that SCBV P2 can bind to both homologous and heterologous nucleic acids in a sequence-
201 nonspecific manner, and the coiled-coil-like domain plays a major role in P2-nucleic acids binding
202 through self-interaction (Lou et al., 2023), and this is consistent with that of CSSV and RTBV
203 (Jacquot et al., 1996; Jacquot et al., 1997). The above results suggest that although the badnaviruses
204 P2 share little sequence similarity, they all possess a conserved coiled-coil-like domain and play
205 an indispensable role in P2-nulceic acids affinity binding, and this property is conserved in
206 badnaviruses and tungroviruses.

Subcellular localization of the SCBV P2 protein

207
208 To determine the precise subcellular localization of SCBV P2, an enhanced green fluorescent
209 protein (eGFP) was fused to the C terminus of P2 (P2-eGFP) and subcloned into the binary
210 expression vector pCHF3 under the transcription of the Cauliflower mosaic virus 35S promoter.
211 *A. tumefaciens* containing the recombinant plasmid pCHF3-P2-eGFP or the pCHF3-eGFP vector
212 were infiltrated into 4- to 5-leaf stage RFP-H2B transgenic *N. benthamiana* plants (containing an
213 RFP nucleus localization signal), respectively. Green fluorescence in inoculum leaves was
214 observed at 2- to 3-dpi using a confocal microscopy. Fluorescence in plants expressing eGFP alone
215 (35S-eGFP) was observed in both cytoplasm and nucleus, and fluorescence in P2-eGFP-infiltrated
216 leaves was also localized in cytoplasm as well as nucleus (Fig. 2A). To further confirm the
217 subcellular localization of P2, the inoculated leaves were digested with cellulase and macerozyme
218 to obtain the protoplasts. The eGFP signal of 35S-eGFP infiltrated mesophyll protoplasts was
219 distributed around the periphery of cytomembrane and nucleus, and it's similar in the 35S-P2-
220 eGFP infiltrated mesophyll protoplasts except some dense bright fluorescent spot (Fig. 2B) The
221 above results indicate P2 have a cytoplasm and nucleus subcellular co-localization.

RNA silencing suppressor activity of SCBV P2

222
223 RNA silencing is an efficient innate antiviral mechanism possessed by plants (Li and Wang, 2019).
224 To repress the transcription of viral DNAs, host Dicer-like protein directs TGS through RdDM, or
225 PTGS, which includes splicing and degradation, or translational repression of recognized viral
226 RNA (Boualem et al., 2016; Matzke and Mosher, 2014). To date, the badnaviruses encoded RNA
227 silencing suppressor (RSS) has been rarely reported. As we described previously that SCBV P2
228 can bind both DNA and RNA (Lou et al., 2023) and is localized in both the cytoplasm and nucleus,
229 suggesting the possibility that it could function as a viral RSS and support viral infection. To test
230 this hypothesis, we used a 16c-transgenic *N. benthamiana* line as the experimental plant, which
231 can constitutively express a green fluorescent protein (GFP) signal localized in the endoplasmic
232 reticulum (ER). *A. tumefaciens* harboring pCHF3-P2 or pCHF3 (negative control) and the p19
233 suppressor encoded by tomato bushy stunt virus (TBSV) (positive control) was individually mixed
234 with an equal volume of *A. tumefaciens* containing a recombinant plasmid expressing the RNA
235 silencing inducer 35S-GFP and inoculated into 4- to 5-leaf aged 16c-transgenic *N. benthamiana*
236 seedlings. By 4 dpi, the strength of green fluorescence in leaves infiltrated with the pCHF3 empty
237 vector had decreased dramatically under UV light, and was almost undetectable under stereo
238 fluorescence microscope, but the intensity remained relatively high in patches expressing P2, and
239 those inoculated with p19 had the highest fluorescence intensity (Fig. 3A), these data indicate that

240   SCBV P2 is an RSS, which can suppress single stranded RNA (ssRNA) triggered local gene
241   silencing.
242   To test whether SCBV P2 can suppress dsRNA-induced gene silencing, wild-type *N.*
243   *benthamiana* plants of 4- to 5-leaf age were infiltrated with *A. tumefaciens* solutions containing
244   the same volume of transient dsRNA elicitor 35S-GFP and 35S-dsFP together with pCHF3,
245   pCHF3-P2, and pCHF3-p19, respectively. As shown in Fig. 3B, leaf spots infiltrated with neither
246   pCHF3 nor pCHF3-P2 mixed with the silencing inducer did not show any GFP fluorescence at 4
247   dpi under UV light or stereo fluorescence microscopy, indicating that P2 fails to suppress dsRNA-
248   induced RNA silencing. In contrast, high intensity of green fluorescence was observed in patches
249   expressing the p19 positive control (Fig. 3B). The above data suggest that SCBV P2 is a weak
250   local ss-PTGS but not a ds-PTGS suppressor.
251   To determine whether P2 can also conquer TGS, a transgenic *N. benthamiana* line named 16-
252   TGS (the CaMV 35S promoter of the GFP transgene is transcriptionally silenced) was used.
253   Transgenic seedlings of 4- to 5-leaf stage were inoculated with GV3101 *A. tumefaciens* solutions
254   (mock) or PVX-P2, PVX (negative control), or PVX-βC1 (the TGS repressor of tomato yellow
255   leaf curl China betasatellite (TYLCCNB), positive control), respectively. After 21 dpi, PVX-
256   infected plants were almost asymptomatic and no visible green fluorescence was detected in
257   systemic tissues under a high intensity UV lamp. However, PVX-βC1-infected plants exhibited
258   severe dwarfing, stem deformation and upward leaf curling along with the PVX-immanent mosaic
259   symptoms, and GFP fluorescence was quite noticeable. As shown in Fig. 3C, systemic leaves
260   infected with PVX-P2 showed severe mosaic and spotty mottling symptoms accompanied with
261   visible green fluorescence under UV light (Fig. 3C), indicating that P2 is a potential TGS repressor.
262   **SCBV P2 expression impacts RdDM signaling in the host**
263   In plants, DNA methylation is a conserved epigenetic modification that regulates genome stability,
264   gene expression, and antiviral defense (He et al., 2022; Wang et al., 2019; Zhang et al., 2018). And
265   the methylation level of the plant host is reprogrammed when challenged by an invading virus. To
266   investigate the effect of P2 on the global methylation patterns of the host plant, we constructed a
267   transgenic P2 line of *N. benthamiana* and tested methylation at the genome level using a
268   methylcytosine-dependent endonuclease (*Mcr*BC). Genomic DNA from pCHF3 (Vec) and P2
269   transgenic *N. benthamiana* plants (5# and 9#) were extracted and subsequently processed with
270   restriction digestion assays. A mock treatment without enzyme was performed as a control (Sham),
271   and all genomic DNA samples remained unaltered. When a methylation-insensitive endonuclease
272   (*Bam*HI) was used, we found that all three genomic DNA samples were digested and formed a
273   'smear' pattern on the agarose gel during electrophoresis (Fig. 4A). However, *Mcr*BC treatment
274   cleaved a portion of the Vec DNA, whereas the DNA from the P2 transgenic lines showed high
275   resistance and remained unchanged (Fig. 4A). The present data suggest that P2 can reduce DNA
276   methylation on a genome-wide scale when transgenically expressed in *N. benthamiana* plants.
277   To explore the possible mechanism of SCBV P2 in repressing epigenetic TGS and genome-
278   wide DNA methylation, the relative expression levels of the homologous genes of DNA
279   methyltransferases, demethylases, histone deacetylase and essential genes related to the RdDM

280 pathway were analyzed in P2 or empty vector transgenic *N. benthamiana* plants. Specific primers
281 were designed and synthesized for qRT-PCR detection of the homologs of DNA
282 methyltransferases (MET1, DRM2 and CMT3), demethylases (ROS1, ROS2), argonautes (AGO1-
283 1, AGO4-1), dicers (DCL3), and histone deacetylase 6 (HDA6). Total RNA from empty vector
284 (Vec) and P2 transgenic *N. benthamiana* plants was extracted 4 weeks after sowing, and total RNA
285 from PVX- or PVX-P2-infected *N. benthamiana* plants was isolated at 15 dpi. The above RNA
286 was reverse transcribed into cDNA and serves as template for the subsequent RT-qPCR assays.
287 As shown in Fig. 4B and 4C, the expression of *Nb*AGO1was significantly down-regulated in both
288 P2 transgenic plants and PVX-P2-infiltrated plants. and the expression of *Nb*AGO4 was
289 dramatically reduced in P2 transgenic *N. benthamiana* plants but remained inconspicuous in PVX-
290 P2-inoculated plants (Fig. 4B and 4C). Surprisingly, we found that the expression level of
291 *Nb*HDA6 was also significantly down-regulated in both P2 transgenic plants and PVX-P2-
292 infiltrated plants, and HDA6 was proved to be a histone deacetylase and cofactor of MET1 that
293 promotes DNA methylation. Taken together, our findings show that P2 consistently
294 overexpression decreases *Nb*AGO1 and *Nb*HDA6 expression so as to suppress host TGS.

295 **SCBV P2 induces a hypersensitive-like response (HLR) in *N. benthamiana*.**
296 SCBV infection usually causes pathchy, chlorotic streaking symptoms (Viswanathan et al., 1996),
297 and induces broken chlorotic streaks in inoculated rice (Bouhida et al., 1993). We successfully
298 constructed an infectious clone of SCBV by inserting a 1.06 copy of the tandem viral genome into
299 the binary vector pCB301-2×35S-HDVRZ-NOS (Fig. S1, A and B). After Agrobacterium-
300 mediated inoculation, SCBV-infected rice seedlings showed stunting and broken chlorotic streaks
301 on leaves at 21 dpi (Fig. S1, C), consistent with the results of Bouhida and colleagues (Bouhida et
302 al., 1993). We also investigated whether the necrotic streaks were the results of a hypersensitive-
303 like response. The rice leaves that showed typical necrotic streaks were stained with 3,3'-
304 diaminobenzidine (DAB), and the mock and pCB301-2×35S-HDVRZ-NOS empty vector
305 infiltrated plants were used as controls. As shown in Fig. S1, brown necrotic spots appeared in
306 leaves infected with SCBV, whereas plants inoculated with mock and empty vector remained
307 transparent and speckless. The accumulation of viral genomic DNA was verified by PCR analysis,
308 and the results indicate that infectious SCBV can successfully infect rice and cause H_2O_2
309 accumulation-induced HLR.
310   To evaluate whether SCBV P2 is a symptom elicitor in *N. benthamiana*, the P2 protein was
311 ectopically overexpressed by a PVX-based vector. *N. benthamiana* plants of 4- to 5-leaf stage were
312 inoculated with *A. tumefaciens* harboring PVX or PVX-P2, respectively. At 7 dpi, PVX-infected
313 plants began to show typical mosaic and shriveling symptoms, whereas PVX-P2-infiltrated plants
314 remained symptomless (Fig. 5A, upper panels). At 10 dpi, the symptoms of PVX-P2-infected
315 plants resembled those of PVX-infected plants (Fig. 5A, middle panels). Symptoms of PVX-
316 infected plants showed signs of recovery from 12 dpi, and vein chlorosis and mosaic phenotype
317 disappeared by 20 dpi, whereas P2-expressing plants still exhibited mosaic and leaf wrinkling
318 phenotypes (Fig. 5A, lower panels). These findings suggest that SCBV P2 can delay the onset of
319 host symptoms to some extent and persist for a considerably longer period of time. To demonstrate

320 the relationship between necrosis and H_2O_2 accumulation, the 3,3'-diaminobenzidine (DAB)
321 staining assay was performed to detect the accumulation of H_2O_2 in empty or PVX-P2 inoculated
322 plants at 10 dpi and 20 dpi, and we found that P2-expressing leaves had many brown necrotic spots
323 at 20 dpi, whereas leaves inoculated with the vector remained spotless (Fig. 5B). Protein
324 immunoblotting analyses confirmed that PVX CP accumulated in greater amounts in PVX-P2-
325 inoculated plants than that in PVX-inoculated plants (Fig. 5C), suggesting that P2 is a potential
326 virulence factor that promotes PVX replication and accumulation. These results indicate that
327 SCBV P2 protein is a viral pathogenicity factor that can induce a hypersensitive-like response and
328 promote virus accumulation.

Discussion

330 Sugarcane bacilliform virus (SCBV)is an important member of *Badnavirus* that causes severe
331 quality and yield losses worldwide. Although many efforts have been made to reveal the molecular
332 characteristics, pathogenicity, and pathogenesis of SCBV, little is clear. We previously
333 demonstrated that the P2 protein of SCBV can bind both viral and heterogenous DNA or RNA in
334 a sequence nonspecific manner (Lou et al., 2023), which is consistent with the findings of CSSV,
335 CoYMV, and RTBV (Cheng et al., 1996; Jacquot et al., 1996; Jacquot et al., 1997). Although the
336 P2 proteins of badnaviruses do not show obvious sequence homology (Fig. 1), they all possess
337 nucleic acid binding activity, which appears to be a universal property of badnaviruses P2 proteins.
338 Furthermore, we have proved that the coiled-coil-like region in P2 is critical for self-interaction
339 and nucleic acid binding (Lou et al., 2023), and the coiled-coil-like region is fairly conserved in
340 size and position among *Badnavirus* and *Tungrovirus*, indicating its universal crucial role for the
341 P2 protein. Since P2 has the ability to bind nucleic acids, it could play a key role in preserving
342 viral nucleic acids from degradation or be involved in virion assembly.

343   RNA silencing is an evolutionarily conserved immune barrier in microbes, such as plant viruses
344 (Li and Wang, 2019). To overcome this defense, viruses have evolved a variety of proteins (such
345 as RSSs) capable of suppressing host gene silencing by other PTGS or TGS via the RdDM pathway
346 (Boualem et al., 2016; Matzke and Mosher, 2014). In general, viral-encoded RSSs are
347 multifunctional and can play critical roles in various stages of the virus infection in addition to
348 suppressing RNA silencing (Csorba et al., 2015; Yang and Li, 2018). For example, CaMV P6 has
349 been proved to act as an RSS by suppressing the activity of DRB4 (Haas et al., 2015). RTBV P4
350 can inhibit the production of siRNA to suppress RNA silencing (Rajeswaran et al., 2014). Here,
351 we tested the PTGS repressor activity of SCBV P2 and found that P2 can inhibit sense RNA-
352 induced but not dsRNA-induced PTGS (Fig. 3), implying that P2 may also repress the formation
353 of dsRNA or degradation but has no effect on siRNA metabolism. In fact, some other
354 Caulimovirus-derived suppressor proteins, such as P6 encoded by strawberry vein banding virus
355 (SVBV), may interfere with dsRNA degradation and act as an RSS (Feng et al., 2018).

356   RdDM is a common epigenetic modification that plays critical roles in gene expression
357 regulation and defense against invading viruses. As a counter-defense strategy, some plant viruses
358 encode TGS suppressors as a tactic to block the activity of essential enzymes or protect the
359 substrates from degradation in the subsequent methylation cycle (Ismayil et al., 2018; Raja et al.,

360 2008; Yang et al., 2011; Zhang et al., 2011). For example, HC-Pro protein from the *Potyviridae*
361 family is involved in lots of processes of RNA silencing suppression by blocking methylation of
362 the 3'-end of siRNA or directly binding to AGO1 and downregulating its expression, etc. (Valli et
363 al., 2018). And the P0 proteins from the genus *Polerovirus* have been shown to block the binding
364 of siRNAs/miRNAs to the free AGO effector to form an intact RNA-induced silencing complex
365 (RISC) and mediate the degradation of AGO1 via the autophagy pathway (Csorba et al., 2010;
366 Michaeli et al., 2019). In this study, we verified that SCBV P2 inhibits TGS by suppressing the
367 expression of AGO1 and AGO4 (Fig. 4B and 4C), which were known to defend against plant RNA
368 viruses (Morel et al., 2002; Wu et al., 2015; Zhang et al., 2006) and DNA viruses (Raja et al.,
369 2008), respectively. AGO1 regulates gene expression in a variety of developmental and
370 physiological processes (Fei et al., 2013; Rogers and Chen, 2013). It also functions in virus defense
371 when loaded with viral siRNAs via dsRNA-triggered gene silencing (Fang and Qi, 2016; Wu et
372 al., 2015), and in this study P2 downregulate the expression level of *Nb*AGO1 but had no visible
373 influence on ds-PTGS (Fig. 3 and 4), although the details remain to be elucidated. The AGO4
374 protein is a crucial component of the RdDM pathway that recruits DRM2, a major de novo
375 methyltransferase, to add methyl to target DNA (Cao and Jacobsen, 2002; Zhong et al., 2014).
376 Furthermore, we found that SCBV P2 transgenic plants showed much lower levels of methylation
377 genome-wide than empty vector transgenic seedlings (Fig. 4A). Taken together, these results
378 provide a model that SCBV P2 represses host DNA methylation by suppressing or disrupting
379 various components involved in the DNA methylation pathway.
380   Oxidative burst (including O^{-2} and H_2O_2) induced HR (Mubin et al., 2010) is universal when
381 plants respond to pathogens and is thought to limit pathogen growth or movement (Hussain et al.,
382 2007; Lam et al., 2001). In this study, we found that SCBV P2 could induce typical mosaic
383 symptoms and HLR necrosis in the late stage of infection with a PVX-based vector (Fig. 5). This
384 suggests that P2 somewhat delays the onset of viral symptoms but triggers H_2O_2 accumulation and
385 causes necrosis symptoms. These results are consistent with the findings of inoculation with
386 infectious clone in *Oryza sativa* (Fig. S1), further confirming that P2 is the pathogenic factor
387 encoded by SCBV. Intriguingly, several plant DNA viruses encoding TGS suppressors have been
388 verified to be virulence factors inducing HR, such as the V2 protein of papaya leaf curl virus
389 (PaLCuV), cotton leaf curl Kokhran virus (CLCuKoV) and tomato leaf curl Java virus (ToLCJV)
390 (Hussain et al., 2007; Mubin et al., 2010; Sharma and Ikegami, 2010). Based on the above results,
391 we suppose that the pathogenesis and TGS repressor activity of SCBV P2 are coupled. Altogether,
392 these observations indicate that SCBV P2 is a multifunctional protein that can suppress PTGS and
393 TGS as well as induce HLR. All these findings help to elucidate the molecular pathogenesis of
394 *Badnavirus* and provide a possible target for future antiviral breeding.
395

Conclusions

397 Our work reveals the fact that the P2 protein encoded by sugarcane bacilliform virus (SCBV) plays
398 an important role in the pathogenicity of the virus, which serves as a ss-PTGS suppressor and
399 represses host TGS by impairing host genome wide DNA methylation level and inhibiting core

400 genes transcription in RdDM pathway, such as AGO1. Besides, P2 was proved to be a virulence
401 factor, which can induce HLR and assist PVX accumulation in *N. benthamiana*. Our conclusions
402 increase the awareness of the molecular mechanism of pathogenesis, as well as help lay a
403 foundation for disease resistance breeding.

404

Acknowledgements

406 We thank professor Xueping Zhou from Institute of Plant Protection, Chinese Academy of
407 Agricultural Sciences for kindly giving the PVX-based expression vector and Mouse anti-PVX CP
408 monoclonal antibody. And we also thank professor Xiaorong Tao from Nanjing Agriculture
409 University for kindly providing the pCB301-2×35S-HDVRZ-NOS binary vector.

410

Additional information and declarations

412

Funding

414 This research was supported by the Natural Science Foundation of Guangxi Province
415 (2023GXNSFBA026058), the Sugarcane Research Foundation of Guangxi University
416 (2022GZB011) and the Innovation Project of Guangxi Graduate Education (YCSW2022065).

417

Grant disclosures

419 The following grant information was disclosed by the authors:
420 Natural Science Foundation of Guangxi Province: 2023GXNSFBA026058.
421 Sugarcane Research Foundation of Guangxi University: 2022GZB011.
422 Innovation Project of Guangxi Graduate Education: YCSW2022065.

Competing interests

424 The authors declare there are no competing interests.

Author contributions

426 Yinian Lou analyzed the data, performed the experiments, prepared figures and/or tables, wrote
427 drafts of the paper, and approved the final draft.
428 Kaili Liang, Jingying Liu and Zhiyuan Wang analyzed the data, performed the experiments,
429 prepared figures and/or tables.
430 Baoshan Chen and Wenlan Li reviewed and revised drafts of the paper.
431 Xiongbiao Xu conceived and designed the experiments, authored or reviewed drafts of the paper,
432 and approved the final draft.

433

434

References

436 Ahmad K, Sun SR, Chen JL, Huang MT, Fu HY, Gao SJ. 2019. Presence of diverse sugarcane
437   bacilliform viruses infecting sugarcane in China revealed by pairwise sequence comparisons
438   and phylogenetic analysis. Plant Pathology Journal 35(1): 41-50. doi:
439   10.5423/PPJ.OA.08.2018.0156.

440 Bhat AI, Hohn T, Selvarajan R. 2016. Badnaviruses: The Current Global Scenario. Viruses
441   8(6):177. doi: 10.3390/v8060177.

442 Boualem A, Dogimont C, Bendahmane A. 2016. The battle for survival between viruses and their
443   host plants. Current Opinion in Virology 17: 32-38. doi: 10.1016/j.coviro.2015.12.001.

444 Bouhida M, Lockhart BE, Olszewski NE. 1993. An analysis of the complete sequence of a
445   sugarcane bacilliform virus genome infectious to banana and rice. Journal of General
446   Virology 74 (Pt 1): 15-22. doi: 10.1099/0022-1317-74-1-15.

447 Cao X, Jacobsen SE. 2002. Role of the arabidopsis DRM methyltransferases in de novo DNA
448   methylation and gene silencing. Current Biology 12(13):1138-1144. doi: 10.1016/s0960-
449   9822(02)00925-9.

450 Cheng CP, Lockhart BE, Olszewski NE. 1996. The ORF I and II proteins of Commelina yellow
451   mottle virus are virion-associated. Virology 223(2): 263-271. doi: 10.1006/viro.1996.0478.

452 Csorba T, Kontra L, Burgyán J. 2015. viral silencing suppressors: Tools forged to fine-tune host-
453   pathogen coexistence. Virology 479-480: 85-103. doi: 10.1016/j.virol.2015.02.028.

454 Csorba T, Lózsa R, Hutvágner G, Burgyán J. 2010. Polerovirus protein P0 prevents the assembly
455   of small RNA-containing RISC complexes and leads to degradation of ARGONAUTE1.
456   Plant Journal 62(3): 463-472. doi: 10.1111/j.1365-313X.2010.04163.x.

457 Davies JP, Reddy V, Liu XL, Reddy AS, Ainley WM, Thompson M, Sastry-Dent L, Cao Z,
458   Connell J, Gonzalez DO, Wagner DR. 2014. Identification and use of the sugarcane
459   bacilliform virus enhancer in transgenic maize. BMC Plant Biology 14: 359. doi:
460   10.1186/s12870-014-0359-3.

461 Fang X, Qi Y. 2016. RNAi in Plants: An Argonaute-Centered View. Plant Cell 28(2): 272-285.
462   doi: 10.1105/tpc.15.00920.

463 Fei Q, Xia R, Meyers BC. 2013. Phased, secondary, small interfering RNAs in posttranscriptional
464   regulatory networks. Plant Cell 25(7): 2400-2415. doi: 10.1105/tpc.113.114652.

465 Feng M, Zuo D, Jiang X, Li S, Chen J, Jiang L, Zhou X, Jiang T. 2018. Identification of Strawberry
466   vein banding virus encoded P6 as an RNA silencing suppressor. Virology 520: 103-110. doi:
467   10.1016/j.virol.2018.05.003.

468 Gao SJ, Damaj MB, Park JW, Wu XB, Sun SR, Chen RK, Mirkov TE. 2017. A novel Sugarcane
469   bacilliform virus promoter confers gene expression preferentially in the vascular bundle and
470   storage parenchyma of the sugarcane culm. Biotechnology for Biofuels 10: 172. doi:
471   10.1186/s13068-017-0850-9.

472 Geijskes RJ, Braithwaite KS, Dale JL, Harding RM, Smith GR. 2002. Sequence analysis of an
473   Australian isolate of sugarcane bacilliform badnavirus. Archives of Virology 147(12):2393-
474   404. doi: 10.1007/s00705-002-0879-2.

475 Haas G, Azevedo J, Moissiard G, Geldreich A, Himber C, Bureau M, Fukuhara T, Keller M,
476   Voinnet O. 2015. Nuclear import of CaMV P6 is required for infection and suppression of
477   the RNA silencing factor DRB4. EMBO Journal 27(15):2102-2112. doi:
478   10.1038/emboj.2008.129.
479 He L, Huang H, Bradai M, Zhao C, You Y, Ma J, Zhao L, Lozano-Duran R, Zhu JK. 2022. DNA
480   methylation-free Arabidopsis reveals crucial roles of DNA methylation in regulating gene
481   expression and development. Nature Communications 13(1): 1335. doi: 10.1038/s41467-
482   022-28940-2.
483 Hussain M, Mansoor S, Iram S, Zafar Y, Briddon RW. 2007. The hypersensitive response to
484   tomato leaf curl New Delhi virus nuclear shuttle protein is inhibited by transcriptional
485   activator protein. Molecular Plant-Microbe Interactions 20(12): 1581-1588. doi:
486   10.1094/MPMI-20-12-1581.
487 Ismayil A, Haxim Y, Wang Y, Li H, Qian L, Han T, Chen T, Jia Q, Yihao Liu A, Zhu S, Deng H,
488   Gorovits R, Hong Y, Hanley-Bowdoin L, Liu Y. 2018. Cotton leaf curl Multan virus C4
489   protein suppresses both transcriptional and post-transcriptional gene silencing by interacting
490   with SAM synthetase. PLoS Pathogens 14(8): e1007282. doi: 10.1371/journal.ppat.1007282.
491 Jacquot E, Hagen LS, Jacquemond M, Yot P. 1996. The open reading frame 2 product of cacao
492   swollen shoot badnavirus is a nucleic acid-binding protein. Virology 225(1): 191-195. doi:
493   10.1006/viro.1996.0587.
494 Jacquot E, Keller M, Yot P. 1997. A short basic domain supports a nucleic acid-binding activity
495   in the rice tungro bacilliform virus open reading frame 2 product. Virology 239(2): 352-359.
496   doi: 10.1006/viro.1997.8859.
497 Johansen LK, Carrington JC. 2001. Silencing on the spot. Induction and suppression of RNA
498   silencing in the Agrobacterium-mediated transient expression system. Plant Physiology
499   126(3), 930-938. doi: 10.1104/pp.126.3.930.
500 Lam E, Kato N, Lawton M. 2001. Programmed cell death, mitochondria and the plant
501   hypersensitive response. Nature 411(6839): 848-853. doi: 10.1038/35081184.
502 Li F, Huang C, Li Z, Zhou X. 2014. Suppression of RNA silencing by a plant DNA virus satellite
503   requires a host calmodulin-like protein to repress RDR6 expression. PLoS Pathogens 10(2):
504   e1003921. doi: 10.1371/journal.ppat.1003921.
505 Li F, Wang A. 2019. RNA-Targeted Antiviral Immunity: More Than Just RNA Silencing. Trends
506   in Microbiology 27 (9):792-805. doi: 10.1016/j.tim.2019.05.007.
507 Li F, Xu X, Huang C, Gu Z, Cao L, Hu T, Ding M, Li Z, Zhou X. 2015. The AC5 protein encoded
508   by Mungbean yellow mosaic India virus is a pathogenicity determinant that suppresses RNA
509   silencing-based antiviral defenses. New Phytologist 208(2): 555-569. doi:
510   10.1111/nph.13473.
511 Liang K, Liu J, BaoY, Wang Z, Xu X. 2023. Screening and identification of host factors interacting
512   with the virulence factor P0 encoded by Sugarcane yellow leaf virus by Yeast two-hybrid
513   assay. Genes 14(7): 1397. doi: 10.3390/genes14071397.

514 Livak KJ, Schmittgen TD. 2001. Analysis of relative gene expression data using real-time
515   quantitative PCR and the 2(-Delta Delta C(T)) Method. Methods 25(4):402-408. doi:
516   10.1006/meth.2001.1262.
517 Lockhart BEL, Irey MJ, Comstock JC. 1995. Sugarcane bacilliform virus, Sugarcane mild mosaic
518   virus and Sugarcane yellow leaf syndrome, Sugarcane Germplasm Conservation &
519   Exchange: Report of An International Workshop Held in Brisbane.
520 Lockhart BEL. 1988. Occurrence in sugarcane of a bacilliform virus related serologically to
521   banana streak virus. Plant Disease 72(3): 230-233. doi:10.1094/PD-72-0230.
522 Lou Y, Liang K, Liu J, Wang Z, Xu X. 2023. Nucleic acid binding activity analysis and key domain
523   identification of Sugarcane bacilliform virus encoded P2 protein. Genomics and Applied
524   Biology (in Chinese). http://kns.cnki.net/kcms/detail/45.1369.Q.20230314.1511.002.html.
525 Matzke MA, Mosher RA. 2014. RNA-directed DNA methylation: an epigenetic pathway of
526   increasing complexity. Nature Reviews Genetics 15(6): 394-408. doi: 10.1038/nrg3683.
527 Michaeli S, Clavel M, Lechner E, Viotti C, Wu J, Dubois M, Hacquard T, Derrien B, Izquierdo E,
528   Lecorbeiller M, Bouteiller N, De Cilia J, Ziegler-Graff V, Vaucheret H, Galili G, Genschik
529   P. 2019. The viral F-box protein P0 induces an ER-derived autophagy degradation pathway
530   for the clearance of membrane-bound AGO1. Proceedings of the National Academy of
531   Science of the United States of America 116(45): 22872-22883. doi:
532   10.1073/pnas.1912222116.
533 Morel JB, Godon C, Mourrain P, Béclin C, Boutet S, Feuerbach F, Proux F, Vaucheret H. 2002.
534   Fertile hypomorphic ARGONAUTE (ago1) mutants impaired in post-transcriptional gene
535   silencing and virus resistance. Plant Cell 14(3): 629-639. doi: 10.1105/tpc.010358.
536 Mubin M, Amin I, Amrao L, Briddon RW, Mansoor S. 2010. The hypersensitive response induced
537   by the V2 protein of a monopartite begomovirus is countered by the C2 protein. Molecular
538   Plant Pathology 11(2): 245-254. doi: 10.1111/j.1364-3703.2009.00601.x.
539 Raja P, Sanville BC, Buchmann RC, Bisaro DM. 2008. Viral genome methylation as an epigenetic
540   defense against geminiviruses. Journal of Virology 82(18): 8997-9007. Viral genome
541   methylation as an epigenetic defense against geminiviruses
542 Rajeswaran R, Golyaev V, Seguin J, Zvereva AS, Farinelli L, Pooggin MM. 2014. Interactions of
543   Rice tungro bacilliform pararetrovirus and its protein P4 with plant RNA-silencing
544   machinery. Molecular Plant-Microbe Interactions 27(12): 1370-1378. doi: 10.1094/MPMI-
545   07-14-0201-R.
546 Rogers K, Chen X. 2013. Biogenesis, turnover, and mode of action of plant microRNAs. Plant
547   Cell 25(7): 2383-2399. doi: 10.1105/tpc.113.113159.
548 Sharma P, Ikegami M. 2010. Tomato leaf curl Java virus V2 protein is a determinant of virulence,
549   hypersensitive response and suppression of posttranscriptional gene silencing. Virology
550   396(1): 85-93. doi: 10.1016/j.virol.2009.10.012.
551 Shen Q, Liu Z, Song F, Xie Q, Hanley-Bowdoin L, Zhou X. 2011. Tomato SlSnRK1 Protein
552   Interacts with and Phosphorylates βC1, a Pathogenesis Protein Encoded by a Geminivirus β-
553   Satellite. Plant Physiology 157(3): 1394-1406. doi: 10.1104/pp.111.184648.

554   Singh D, Tewari AK, Rao GP, Karuppaiah R, Viswanathan R, Arya M, Baranwal VK. 2009. RT-
555   PCR/PCR analysis detected mixed infection of DNA and RNA viruses infecting sugarcane
556   crops in different states of India. Sugar Tech 11(4): 373-380. doi:10.1007/s12355-009-0064-
557   y.
558   Springer NM. 2010. Isolation of plant DNA for PCR and genotyping using organic extraction and
559   CTAB. Cold Spring Harbor Protocols. 2010(11):pdb.prot5515. doi: 10.1101/pdb.prot5515.
560   Sun SR, Damaj MB, Alabi OJ, Wu XB, Mirkov TE, Fu HY, Chen RK, Gao SJ. 2016. Molecular
561   characterization of two divergent variants of sugarcane bacilliform viruses infecting
562   sugarcane in China. European Journal of Plant Pathology 145(2):375-384.
563   doi:10.1007/s10658-015-0851-0.
564   Valli AA, Gallo A, Rodamilans B, Lopez-Moya JJ, Garcia JA. 2018. The HCPro from the
565   Potyviridae family: an enviable multitasking Helper Component that every virus would like
566   to have. Molecular Plant Pathology 19(3): 744-763. doi: 10.1111/mpp.12553.
567   Viswanathan R, Alexander KC, Garg ID. 1996. Detection of sugarcane bacilliform virus in
568   sugarcane germplasm. Acta Virologica 40(1): 5-8.
569   Viswanathan R, Premachandran MN. 1998. Occurrence and distribution of sugarcane bacilliform
570   virus in the sugarcane germplasm collection in India. Sugar Cane (United Kingdom).
571   Voinnet O, Baulcombe DC. 1997. Systemic signalling in gene silencing. Nature 389(6651): 553.
572   doi: 10.1038/39215.
573   Wang C, Wang C, Zou J, Yang Y, Li Z, Zhu S. 2019. Epigenetics in the plant-virus interaction.
574   Plant Cell Reports 38(9): 1031-1038. doi: 10.1007/s00299-019-02414-0.
575   Wu J, Yang Z, Wang Y, Zheng L, Ye R, Ji Y, Zhao S, Ji S, Liu R, Xu L, Zheng H, Zhou Y, Zhang
576   X, Cao X, Xie L, Wu Z, Qi Y, Li Y. 2015. Viral-inducible Argonaute18 confers broad-
577   spectrum virus resistance in rice by sequestering a host microRNA. eLife 4, e05733. doi:
578   10.7554/eLife.05733.
579   Xiong R, Wu J, Zhou Y, Zhou X. 2009. Characterization and subcellular localization of an RNA
580   silencing suppressor encoded by Rice stripe tenuivirus. Virology 387(1):29-40. doi:
581   10.1016/j.virol.2009.01.045.
582   Yang X, Xie Y, Raja P, Li S, Wolf JN, Shen Q, Bisaro DM, Zhou X. 2011. Suppression of
583   methylation-mediated transcriptional gene silencing by βC1-SAHH protein interaction during
584   geminivirus-betasatellite infection. PLoS Pathogens 7(10): e1002329. doi:
585   10.1371/journal.ppat.1002329.
586   Yang Z, Li Y. 2018. Dissection of RNAi-based antiviral immunity in plants. Current Opinion in
587   Virology 32: 88-99. doi: 10.1016/j.coviro.2018.08.003.
588   Yoo SD, Cho YH, Sheen J. 2007. Arabidopsis mesophyll protoplasts: a versatile cell system for
589   transient gene expression analysis. Nature Protocols 2(7): 1565-1572. doi:
590   10.1038/nprot.2007.199.
591   Zhang H, Lang Z, Zhu JK. 2018. Dynamics and function of DNA methylation in plants. Nature
592   Reviews Molecular Cell Biology 19(8): 489-506. doi: 10.1038/s41580-018-0016-z.

593 Zhang X, Yuan YR, Pei Y, Lin SS, Tuschl T, Patel DJ, Chua NH. 2006. Cucumber mosaic virus-
594   encoded 2b suppressor inhibits Arabidopsis Argonaute1 cleavage activity to counter plant
595   defense. Genes & Development 20(23): 3255-3268. doi: 10.1101/gad.1495506.
596 Zhang Z, Chen H, Huang X, Xia R, Zhao Q, Lai J, Teng K, Li Y, Liang L, Du Q, Zhou X, Guo H,
597   Xie Q. 2011. BSCTV C2 attenuates the degradation of SAMDC1 to suppress DNA
598   methylation-mediated gene silencing in Arabidopsis. Plant Cell 23(1): 273-288. doi:
599   10.1105/tpc.110.081695.
600 Zhong X, Du J, Hale CJ, Gallego-Bartolome J, Feng S, Vashisht AA, Chory J, Wohlschlegel JA,
601   Patel DJ, Jacobsen SE. 2014. Molecular mechanism of action of plant DRM de novo DNA
602   methyltransferases. Cell 157(5): 1050-1060. doi: 10.1016/j.cell.2014.03.056.
603
604

Amino acid sequences of P2 from sugarcane bacilliform virus (SCBV) and representatives within genus *Badnavirus* and *Tungrovirus*

[a] BSOLV, Banana streak OL virus; CLNV, Cycad leaf necrosis virus; CoYMV, Commelina yellow mottle virus; CSSV, Cacao swollen shoot virus; PYMoV, Piper yellow mottle virus; RTBV, Rice tungro bacilliform virus; SCBV, Sugarcane bacilliform virus; TaBCHV, Taro bacilliform CH virus.

1   **TABLES**

3   **TABLE 1.** Amino acid sequences of P2 from sugarcane bacilliform virus (SCBV) and representatives within

4   genus *Badnavirus* and *Tungrovirus*

Virus [a]	Genus	GenBank accession number	Size (aa)	Amino acid sequence identity (%)
SCBV	*Badnavirus*	WON00947	123	-
BSOLV	*Badnavirus*	NP_569149	135	26.8
CLNV	*Badnavirus*	YP_002117530	128	31.1
CoYMV	*Badnavirus*	NP_039819	136	19.5
CSSV	*Badnavirus*	NP_041733	133	24.6
PYMoV	*Badnavirus*	AXG50781	159	23.8
TaBCHV	*Badnavirus*	YP_009130663	126	28.3
RTBV	*Tungrovirus*	AAD30189	111	22.9

6   [a] BSOLV, Banana streak OL virus; CLNV, Cycad leaf necrosis virus; CoYMV, Commelina yellow mottle virus;

7   CSSV, Cacao swollen shoot virus; PYMoV, Piper yellow mottle virus; RTBV, Rice tungro bacilliform virus;

8   SCBV, Sugarcane bacilliform virus; TaBCHV, Taro bacilliform CH virus.

Figure 1

Figure 1. Phylogenetic relationships between SCBV and other taxa in the genus *Badnavirus* and *Tungrovirus*.

(A) Multiple alignment of amino acid sequence of SCBV P2 and representatives of *Badnavirus* and *Tungrovirus.* The conserved motifs were highlighted and the coiled coil like domain were framed in a rectangle. (B) Unrooted neighbor-joining phylogenetic tree reconstructed from the alignment of the amino acid sequences of SCBV P2 and other taxa in the genus *Badnavirus* and *Tungrovirus.* The phylogenetic tree was constructed by using the MEGA7.0 program and the percentage of bootstrap values (1,000 replicates) are shown at the branch internodes. BSOLV, Banana streak OL virus; CLNV, Cycad leaf necrosis virus; CoYMV, Commelina yellow mottle virus; CSSV, Cacao swollen shoot virus; PYMoV, Piper yellow mottle virus; RTBV, Rice tungro bacilliform virus; SCBV, Sugarcane bacilliform virus; TaBCHV, Taro bacilliform CH virus.
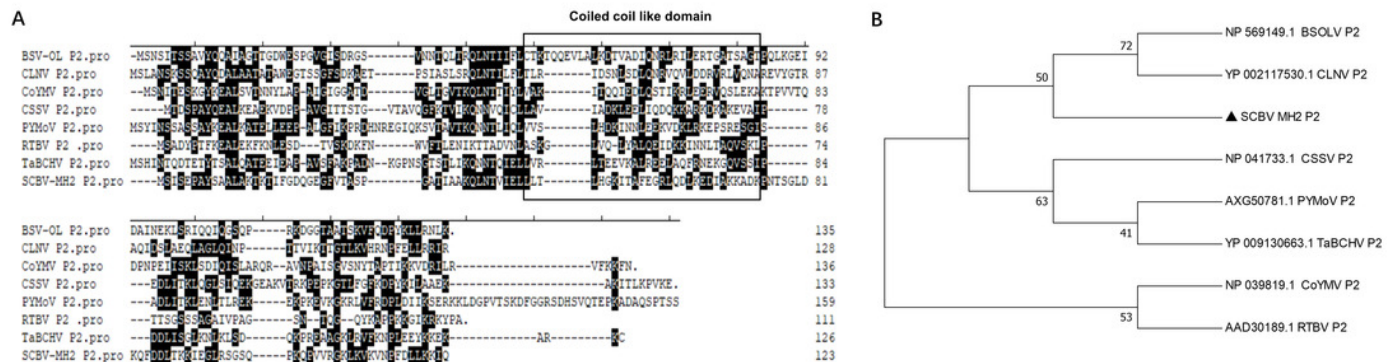
Figure 2

Figure 2. Subcellular localization of SCBV P2 in RFP-H2B transgenic *Nicotiana benthamiana* mesophyll cells and protoplasts.

(A) Subcellular localization of P2 fused to the enhanced green fluorescent protein (eGFP) in RFP-H2B transgenic *N. benthamiana* mesophyll cells. (B) Subcellular localization of P2 fused to eGFP in RFP-H2B transgenic *N. benthamiana* protoplasts. The 35S-eGFP expression plasmid was used as a control. The ratio scale was shown in the bottom right corner of the picture.
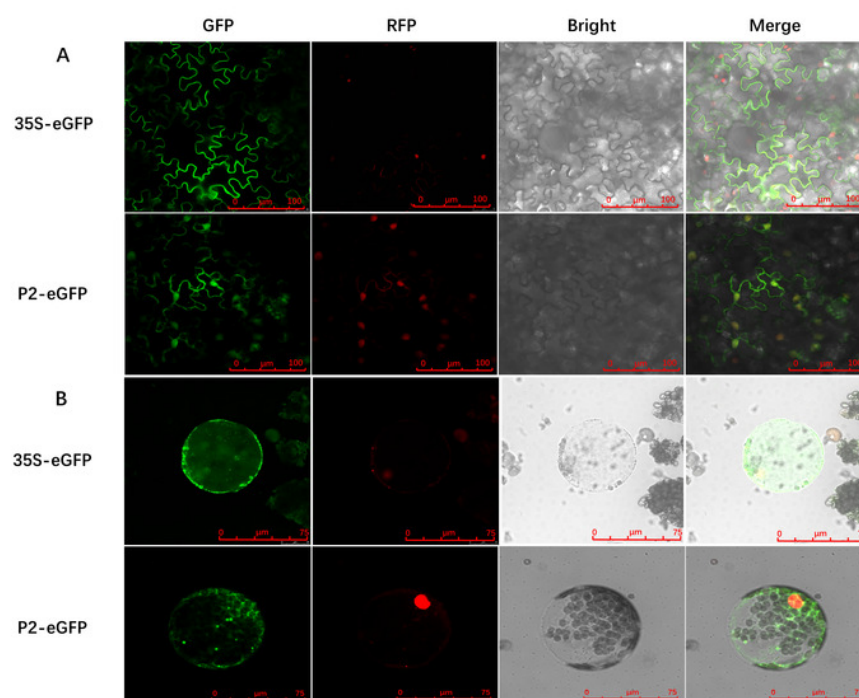
Figure 3

Figure 3. SCBV P2 inhibits ssRNA induced PTGS and reverses TGS.

(A) Repression of GFP silencing in *N. benthamiana* 16c leaves. Leaf areas were co-infiltrated with *A. tumefaciens* expressing GFP (35S-GFP) and either a pCHF3 control, SCBV P2 (pCHF3-SCBV-P2), or TBSV p19 (pCHF3-p19). Photos of the above infiltrated leaves were taken at 4 dpi, under high intensity UV light. (B) Leaf patches of *N. benthamiana* were co-infiltrated with *A. tumefaciens* carrying GFP (35S-GFP) and dsFP (35S-dsFP), as well as pCHF3 vector, SCBV P2 or p19, and typical leaf patches were photographed under high intensity UV light at 4 dpi. (C) Plant of *N. benthamiana* 16-TGS were left uninoculated, or inoculated with PVX, PVX-P2, or PVX- β C1, respectively, and the apex of plants and leaves were photographed under high intensity UV light at 21 dpi.
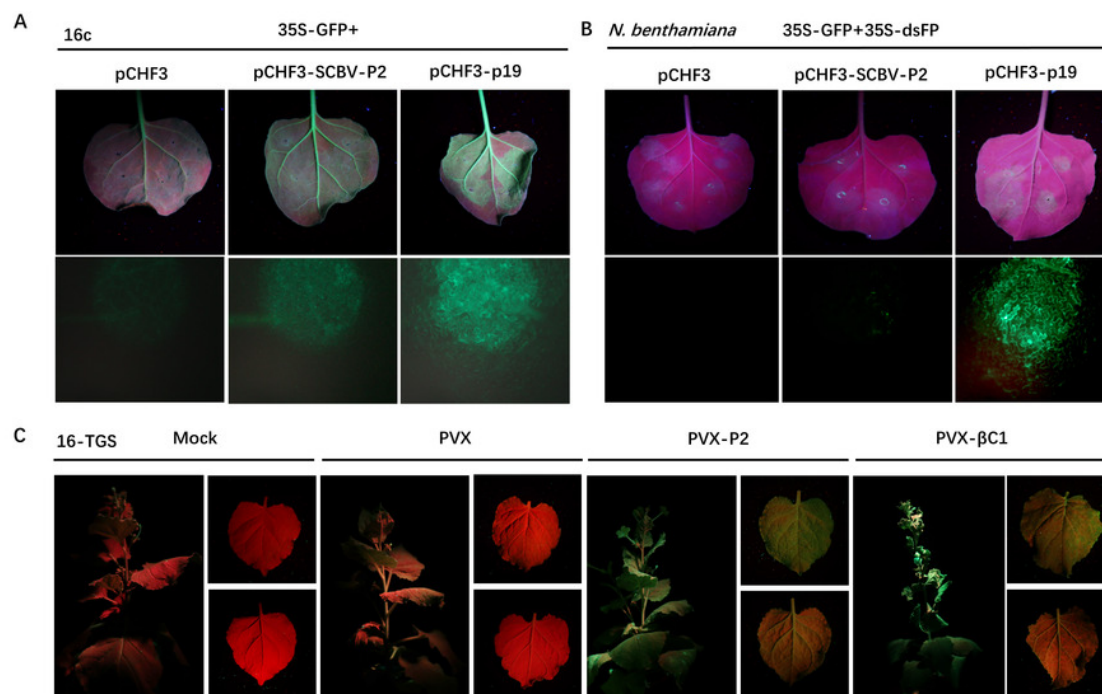
Figure 4

Figure 4. SCBV P2 expression impacts host RdDM pathway andgenome-wide scale methylation.

(A) DNA methylation analysis in P2 transgenic *N. benthamiana* plants using restriction endonuclease digestion. The methylation-dependent endonuclease *Mcr*BC and the methylation-insensitive enzyme BamHI were used to digest genomic DNA isolated from the vector control (Vec) and two separate lines of P2 transgenic plants (5# and 9#). The term 'Sham' refers to a simulated digestion that contains no enzyme. The positions of the uncut input and the digested products are shown. (B) SCBV P2 Overexpression inhibits transcription of *N. benthamiana* ARGONAUTE 1 (*Nb*AGO1) and *Nb*AGO4 in PVX-treated plants. RT-qPCR assays were performed to analyze the effects of P2 on the expression of homologous genes of DNA methyltransferases, demethylases, histone deacetylase and essential genes related to RdDM. Relative expression levels of DNA METHYLTRANSFERASE1 (*Nb*MET1)(GenBank accession number: FJ222441), DOMAINS REARRANGED METHYLTRANSFERASE2 (*Nb*DRM2) (JQ957857), CHROMOMETHYLASE3 (*Nb*CMT3) (JQ957858) , DICER3 (*Nb*DCL3) (FM986782), REPRESSOR OF SILENCING 1 (*Nb*ROS1) (JQ957859), *Nb*ROS2 (JQ957860), *Nb*AGO1 (DQ321488), *Nb*AGO4 (DQ321490) and Histone Deacetylase 6 (*Nb*HDA6) (KU170188) were measured in PVX and PVX-P2 inoculated *N. benthamiana* plants at 15 dpi (B), or in pCHF3 vector and P2 transgenic plants at 30 days after sprouting(C). T-tests were performed to analyze the significance of difference (*P<0.05, **P<0.01). Each of the experiments were carried out at least three times.
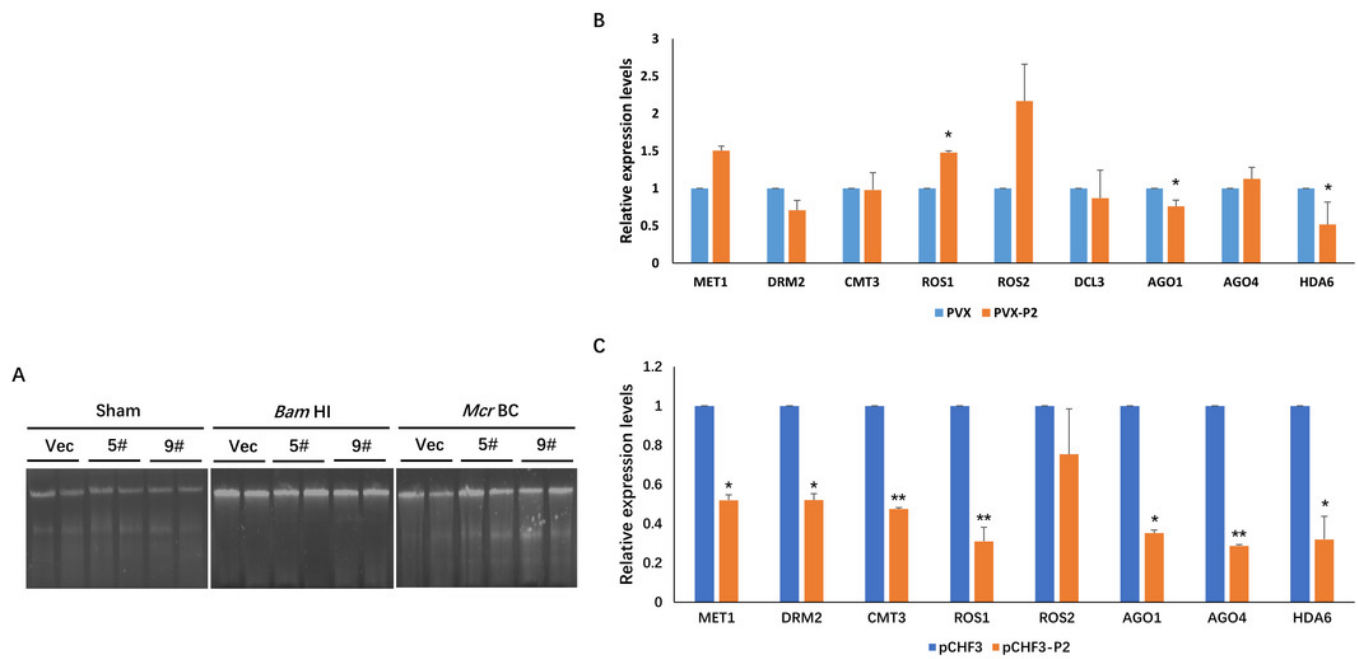
Figure 5

Figure 5. Symptoms of the plants inoculated with Potato virus X(PVX) or PVX-P2.

(A) Symptoms evoked on *N. benthamiana* plants at 7-, 10- and 20-dpi inoculated with PVX or PVX-P2. (B) PVX-P2 induced mosaic symptoms and necrotic spots on *N. benthamiana* plants. Upper systemic leaves were photographed at 10- and 20-dpi, respectively. Followed by photographing after 3,3'-diaminobenzidine (DAB) treatment. The necrotic lesions are shown by the red arrowheads. (C) Western blot analysis of coat protein (CP) accumulation in PVX or PVX-P2 infected plants. Freshly emerging leaves were used to extract total protein. The anti-PVX CP monoclonal antibody was used to detect the accumulation of PVX, Coomassie light blue stained Rubisco large subunit protein was used as a loading control. The gray values of the blot bands were evaluated by using the ImageJ software, the relative amount of CP accumulation in PVX-infected plants was preset as 100%.